Evaluation of geometrical distortion in a head-sized phantom at ultra-high-field (7 Tesla) MRI

P. Dammann[1], O. Kraff[2], S. Maderwald[2], E. Gizewski[3], M. Ladd[2], and T. Gasser[4]

[1]Neurosurgery, University of Duisburg-Essen, Germany and Erwin L. Hahn Institute for Magnetic Resonance Imaging, Essen, NRW, Germany, [2]Erwin L. Hahn Institute for Magnetic Resonance Imaging, [3]Department for Diagn. and Interv. Radiology and Neuroradiology, University of Duisburg-Essen, Germany, [4]Department of Neurosurgery, University of Duisburg-Essen, Germany

Introduction: Geometrical distortion is a well known problem in MRI, leading to pixel shifts [1] with variations up to several millimeters, thereby interfering with precise localization of anatomic structures [2]. Main geometrical inaccuracies are due to hardware (static field inhomogeneity, gradient field nonlinearity, presence of eddy currents caused by gradient switching) and object characteristics (chemical shift, susceptibility effects, flow) [3]. Manufacturer developed distortion correction and shimming procedures are usually applied to decrease geometrical inaccuracies; however, it has been shown that despite these measures distortion can be significant [4,5]. As field inhomogenity, susceptibility, and chemical shift are proportional to B_0, distortions of spatial encoding in MRI tend to increase with higher magnetic field strength. With the upcoming prospects of applying ultra-high-field MRI (B_0 ≥7 Tesla) for neuroimaging and image-guided therapy in neurosurgery [6,7], evaluation of the geometrical distortion in ultra-high-field MRI is an essential precondition. Therefore, we conducted a study to determine system related geometrical distortion in a head-sized phantom at 7 Tesla and compared results to findings at 1.5 Tesla and values reported in previous literature.

Methods: We used a cylindrical MRI head phantom (Elekta, Sweden) equipped with a three-dimensional inlay grid (ø 170.5 mm) with exactly known physical dimensions (Fig. A). Inside the volume there are n=190 defined grid marker points clearly visible on CT and MRI. Distance of these marker points to the volume center range from 15 to 91 mm. For scanning, the phantom was filled with oil. As CT images generally have negligible distortion, initially a CT scan (120 kVp, 512x512 mm², slice thickness 0.75 mm, 216 slices) of the head phantom was performed as reference. Afterwards the phantom was scanned at 1.5 and 7 Tesla field strength (Magnetom Avanto and Magnetom 7 T, Siemens Healthcare, Erlangen, Germany) using clinically relevant gradient echo and spin echo sequences (MPRAGE, FLASH, T2, SWI, for detailed scan parameters see Fig. B). Both MR scanners were equipped with the same gradient coil capable of 45 mT/m maximum amplitude and a slew rate of 220 mT/m/ms. Images were acquired with (2D, 3D) and without distortion correction. After image acquisition the marker points (defined as x_n, y_n, z_n) of the phantom were manually determined using image thresholding and multifold magnification in sub-pixel resolution. The resulting 190 coordinates assessed in each MRI sequence were then referenced to the coordinates assessed in the CT scan. The positional deviations (CT vs. MRI) at each marker point, taken as the MRI related spatial distortion, were computed by the Euclidean distance of each coordinate pair. Marker localization error, as a parameter of reproducibility, was determined by calculating the variance of repetitive (n=10) marker assessments in all three modalities. Image processing was done with the ITK© based Free Open Source Software 3D Slicer (Version 3.4, www.slicer.org) and in-house software based on R2009a-Matlab (MathWorks Inc, USA).

Results: Overall we found very low mean system-related geometrical distortion at both 7 T and 1.5 Tesla, although single values up to 1.5 mm were detected. No major differences in mean distortion between sequences could be found, except significantly higher distortion in T2 imaging at 7 Tesla, though local maxima of distortion differed significantly. Image distortion correction did not improve mean distortion over the entire phantom volume (≤ 91 mm from magnetic center) but did reduce local maxima at the borders of the volume. Detailed information for 7T imaging is given in Fig. C. As marker localization error was ~ 0.2 mm (CT), ~ 0.3 mm (1.5 T) and ~ 0.3 mm (7 T), assessment of positional deviations in this study design seems to be accurate and reliable. This is also reflected by the homogenous distribution of $\Delta_{x,y,z}$ over the volume, with increasing values near the periphery of the phantom (See Fig. D). As expected, pronounced object related artifacts (susceptibility effects, chemical shift) were found in 7T images, but didn't interfere with the marker localization procedure.

Discussion: We present an accurate and reproducible method to assess geometrical distortion. Mean system related geometrical distortion over a head-sized phantom at 7T MRI is lower than expected. This can be explained by the relation of magnetic center position, phantom volume, and FOV. Near the magnetic center the manufacturer warrants high geometrical accuracy. 2D and 3D distortion correction algorithms basically correct for gradient non-linearity and are primarily effective for large FOVs, making them of low relevance for a head-sized phantom (max. distance to magnetic center 91 mm). However, distortion correction did reduce local maxima of distortion. Object related artifacts at 7 T were significant, particularly so called “blooming effects” of susceptibility at SWI. This may lead to much higher inaccuracies in patients.

A

	1.5 Tesla				7 Tesla			
	MPRAGE	VIBE	T2	SWI	MPRAGE	VIBE	T2	SWI
Repetition Time TR [msec]	2180	4.77	4570	49	3500	5	4520	29
Echo Time TE [msec]	3.09	1.92	146	40	2.49	2.04	112	15.2
Inversion Time TI [msec]	1100				1100			
Flip Angle FA [°]	10	12	150	15	10	12	125	25
Field of View FOV [mm²]	256	256	220	256	256	256	220	256
Acquisition Matrix [pixel]	256x256	256x256	256x512	256x256	256x256	245x256	256x512	896x896
Bandwidth [Hz/Pixel]	130	490	70	75	725	725	515	140
Slices	240	224	80	60	256	256	86	88

B

			Δx [mm]			Δy [mm]			Δz [mm]			RMS (Δ_{xyz}) [mm]	
Acquisition	DC	Range	Mean	SD	Range	Mean	SD	Range	Mean	SD	Mean	SD
7 T MPRAGE	n/a	0 – 1.5	0.49	±0.1	0 – 0.9	0.38	±0.3	0 – 1.1	0.51	±0.1	0.62	±0.1
MPRAGE	2D	0 – 1.1	0.41	±0.3	0 – 0.8	0.31	±0.1	0 – 0.7	0.24	±0.2	0.57	±0.1
MPRAGE	3D	0 – 1.2	0.4	±0.2	0 – 0.8	0.31	±0.1	0 – 0.7	0.21	±0.1	0.54	±0.1
FLASH	n/a	0 – 0.5	0.2	±0.1	0 – 0.8	0.34	±0.2	0 – 0.4	0.14	±0.1	0.49	±0.1
FLASH	2D	0 – 0.5	0.22	±0.1	0 – 0.8	0.31	±0.2	0 – 0.6	0.23	±0.2	0.51	±0.1
FLASH	3D	0 – 0.5	0.22	±0.1	0 – 0.7	0.32	±0.2	0 – 0.6	0.22	±0.1	0.51	±0.1
T2	n/a	0 – 1.2	0.53	±0.3	0 – 1.6	0.61	±0.4	0.2-1.4	0.6	±0.2	0.74	±0.1
T2	2D	0 – 1.3	0.51	±0.2	0 – 1.5	0.63	±0.3	0 – 1.4	0.69	±0.2	0.78	±0.1
SWI	n/a	0 – 0.5	0.2	±0.1	0 – 0.6	0.27	±0.2	0 – 0.8	0.41	±0.2	0.55	±0.1
SWI	2D	0 – 0.6	0.23	±0.2	0 – 0.8	0.25	±0.2	0 – 0.6	0.22	±0.1	0.49	±0.1
SWI	3D	0 – 0.4	0.16	±0.1	0 – 1.0	0.34	±0.1	0 – 0.7	0.19	±0.2	0.47	±0.1

C

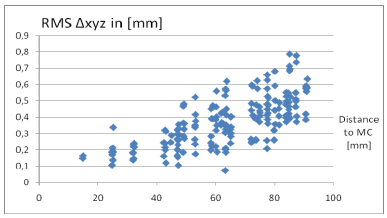

D

Figures: ***A*** *MRI Phantom (Elekta, Sweden).* ***B*** *Scan parameters of MRI sequences at 1.5 and 7 Tesla.* ***C*** *Positional deviations (~ geometrical distortion) in L-R (Δx), A-P (Δy) and H-F (Δz) direction. Cumulative radial distortion as root mean square error (RMS). All values as range, mean, and standard deviation (SD) in [mm]. DC= Distortion correction.* ***D*** *RMS vs. distance to magnetic center. Here a T2 sequence (2D DC) at 7 Tesla. Note the increasing distortion up to 0.8 mm at the borders of the phantom.*

References:

1. Walton L, Hampshire A, Forster DMC, Kemeny AA: A Phantom study to assess the accuracy of stereotactic localization, using T1 weighted magnetic resonance imaging with the Leksell stereotactic system. Neurosurgery 38:170-178, 1996
2. Sumanaweera TS, Glover G, Song S, Adler J, Napel S: Quantifying MRI geometric distortion in tissue. Magn Reson Med 31:40-47, 1994
3. Archip N et al.: Compensation of geometrical distortion effects on intraoperative magnetic resonance imaging for enhanced visualization in image-guided neurosurgery. Neurosurgery 62:209-216, 2008
4. Wang D, Strugnell W, Cowin G, Doddrell DM, Slaughter R: Geometric distortion in clinical MRI systems Part I: Evaluation using a 3D phantom. Magn Reson Imaging 22:1211-1221, 2004
5. Wang D, Strugnell W, Cowin G, Doddrell DM, Slaughter R: Geometric distortion in clinical MRI systems Part II: Correction using a 3D phantom. Magn Reson Imaging 22:1223-1232, 2004
6. Ladd, ME: High-field-strength magnetic resonance: potential and limits. Top Magn Reson Imaging. 2007 Apr;18(2):139-52. Review.